

# Development of Model for Shear-Wave Velocity of Municipal Solid Waste

Dimitrios Zekkos, M.ASCE<sup>1</sup>; Andhika Sahadewa, S.M.ASCE<sup>2</sup>; Richard D. Woods, Dist.M.ASCE<sup>3</sup>; and Kenneth H. Stokoe II, F.ASCE<sup>4</sup>

**Abstract:** The shear-wave velocity and associated small-strain shear modulus of municipal solid waste (MSW) are important engineering parameters in evaluating the seismic response of MSW landfills as well as in characterizing the waste material and its response to static loads. Semiempirical and empirical models for the shear-wave velocity are presented. The semiempirical model is a more comprehensive model that aims to separately capture the effect of waste density and confining stress on the shear-wave velocity of MSW. It is based on similar models for soils, and its mathematical expression is formulated using data generated from large-scale laboratory studies on reconstituted MSW. The empirical model has a simpler mathematical expression that is a function of depth only. The parameters of both models are derived by calibrating them against a total of 49 in situ shear-wave velocity profiles at 19 MSW landfills, i.e., 13 profiles from four landfills in Michigan generated as part of this study and 36 additional shear-wave velocity profiles from 15 landfills available in the literature. The models can be used to estimate the shear-wave velocity of MSW and to evaluate the seismic response of landfills. Also, in the absence of in situ data, the models can be used at existing MSW landfills for preliminary design purposes. The models are not intended to replace in situ data and do not predict abrupt changes in the shear-wave velocity profile as a result of abrupt changes in waste type and composition. DOI: 10.1061/(ASCE)GT.1943-5606.0001017. © 2013 American Society of Civil Engineers.

**Author keywords:** Municipal solid waste; Landfills; Dynamic properties; Field measurements; Shear-wave velocity; Small-strain shear modulus; Multichannel analysis of surface waves; Microtremor analysis method.

## Introduction

The shear-wave velocity is an important engineering property of any material. Factors that affect the shear-wave velocity ( $V_s$ ) of earth materials in the laboratory have been studied extensively (Richart 1975; Hardin and Drnevich 1972), and significant advances have been made in recent years in reliably measuring  $V_s$  in the field (e.g., Stokoe et al. 1994; Stokoe and Santamarina 2000; Rosenblad et al. 2007; Foti et al. 2009; Yoon and Rix 2009; Cox and Beekman 2011; Pelekis and Athanasopoulos 2011). The shear-wave velocity is related to the small-strain shear modulus ( $G_{\max}$ ) using elasticity theory

$$G_{\max} = \rho V_s^2 \quad (1)$$

where  $\rho$  = mass density of the material (equal to the total unit weight of the material,  $\gamma_t$ , divided by the gravitational acceleration). The shear-wave velocity can be used to characterize the stiffness of earth materials and is a critical input parameter in seismic analyses (Kramer 1994). The shear-wave velocity has been used as an index parameter to characterize settlement behavior (Sheehan et al. 2010) as well as the liquefaction susceptibility of granular soils (Andrus and Stokoe 2000; Youd et al. 2001). Previous numerical studies of municipal solid waste (MSW) landfills have shown that variation of  $V_s$  with depth has a significant impact on the results of seismic site response analyses (Augello et al. 1995; Kavazanjian and Matasovic 1995; Athanasopoulos-Zekkos et al. 2008).

Empirical and semiempirical models to estimate the field  $V_s$  of MSW are presented here. A semiempirical model for  $V_s$  that is a function of the effective stress and total unit weight is formulated using large-scale laboratory data on reconstituted MSW. The laboratory data provide the opportunity to understand some of the key factors that affect  $V_s$  of MSW. The model is then calibrated against field measurements of  $V_s$  at MSW landfills in the United States and abroad. An empirical mathematically simpler model is also presented. The calibrated models can be used for preliminary estimates of field  $V_s$  of MSW in the absence of in situ measurements.

## Review of Field $V_s$ Measurements in MSW

The following in situ seismic methods have been used to measure  $V_s$  of MSW:

- Downhole seismic testing (Sharma et al. 1990);
- Crosshole seismic testing (Singh and Murphy 1990);
- Suspension logging (Matasovic and Kavazanjian 1998); and
- The spectral analysis of surface waves (SASW) method (Kavazanjian et al. 1996).

<sup>1</sup>Assistant Professor, Dept. of Civil and Environmental Engineering, Univ. of Michigan, 2350 Hayward St., Ann Arbor, MI 48109 (corresponding author). E-mail: zekkos@geoengineer.org

<sup>2</sup>Graduate Student, Dept. of Civil and Environmental Engineering, Univ. of Michigan, 2350 Hayward St., Ann Arbor, MI 48109. E-mail: sahadewa@umich.edu

<sup>3</sup>Professor Emeritus, Dept. of Civil and Environmental Engineering, Univ. of Michigan, 2350 Hayward St., Ann Arbor, MI 48109. E-mail: rdw@umich.edu

<sup>4</sup>Professor, Dept. of Civil, Architectural and Environmental Engineering, Univ. of Texas at Austin, 301 E. Dean Keeton St., Austin, TX 78712. E-mail: k.stokoe@mail.utexas.edu

Note. This manuscript was submitted on October 16, 2011; approved on July 29, 2013; published online on July 31, 2013. Discussion period open until April 29, 2014; separate discussions must be submitted for individual papers. This paper is part of the *Journal of Geotechnical and Geoenvironmental Engineering*, © ASCE, ISSN 1090-0241/04013030(14)/\$25.00.

Surface wave methods have become increasingly popular for  $V_s$  profiling at MSW landfills because they are nonintrusive (i.e., they do not require drilling), are rapidly performed in the field, and are reliable. The most common surface wave method that has been used at MSW landfills is the SASW (Stokoe et al. 1994). To the authors' knowledge, implementation of other surface wave methods in MSW landfills, such as the multichannel analysis of surface waves (MASW) method (Park et al. 1999a), has not been reported in the literature. In addition, although passive methods (Okada 2003) are increasingly used in engineering practice, they have not been used in landfills. The field measurements of  $V_s$  in landfills available in the literature are described in more detail subsequently. Given the importance of the variation of  $V_s$  with depth in seismic analyses, the focus of this paper is on field data that capture that variation using surface wave methods as opposed to average  $V_s$  values over the entire depth of waste. Table 1 gives a list of MSW  $V_s$  profiles available in the literature.

Kavazanjian et al. (1995) reported  $V_s$  data from various landfills and recommended a  $V_s$  profile for use in seismic analysis of MSW landfills; their profile, shown as open circles, is included in Fig. 1. Kavazanjian et al. (1996) reported results of additional surveys performed with the SASW method. Tests were performed at the Operation Industries (OII), landfill, Azusa Land Reclamation Company landfill, Sunshine Canyon landfill, Lopez Canyon landfill, Toyon Canyon landfill, and an unidentified landfill named Landfill A. A total of 27 SASW  $V_s$  profiles were performed at the OII landfill. SASW tests were also performed at six locations in the Azusa landfill, and at eight locations at the four remaining landfills. Based on these investigations, Kavazanjian et al. (1996) recommended the ranges for  $V_s$  profiles for MSW in southern California shown in Fig. 1.

Cuellar et al. (1998) performed the SASW method at the Villalba waste dump, near Madrid, Spain. The Villalba waste had a  $V_s$  value of about 100 m/s near the surface, reaching a  $V_s$  value of about 210 m/s at a depth of 15 m. Rix et al. (1998) performed SASW tests at two MSW landfills in Atlanta, Georgia. Using simultaneous inversion of surface wave velocity and attenuation measurements, Rix et al. (1998) estimated both the  $V_s$  profile as well as the small-strain

material damping profiles for the Sanifill and Bolton landfills. Kavazanjian (1999) recommended that, in the absence of site-specific data, the southern California profile reported by Kavazanjian et al. (1996) may provide a good representation of  $V_s$  at MSW landfills in temperate and arid climates. Pereira et al. (2002) measured  $V_s$  using the SASW method in the Valdemingomez landfill near Madrid, Spain. In the upper meter, a crust (i.e., a high  $V_s$  layer at the surface overlying layers with lower  $V_s$ ) with  $V_s$  equal to 210 m/s was identified. Below the crust, the  $V_s$  ranged from 100 m/s near the surface to 250 m/s at depth. Lin et al. (2004) performed SASW tests at 14 locations at the Tri-Cities landfill, Altamont landfill, and Redwood landfill in northern California. A handheld hammer was used to generate higher-frequency waves to evaluate  $V_s$  near the surface, and a tract-type tractor was used to generate lower-frequency waves that allowed evaluation of  $V_s$  to depths reaching 30 m. The profiles at all northern California locations appeared to be similar and are also shown in Fig. 1. Matasovic and Kavazanjian (2006) reported the use of the SASW method to measure  $V_s$  at three locations at the Olympic View Sanitary Landfill (OVSL) near Port Orchard, Washington, where  $V_s$  was found to vary from about 80–200 m/s near the surface to about 250 m/s at a depth of 20 m.

### Factors Affecting $V_s$ of MSW Based on Laboratory Studies

There are three large-scale laboratory studies on the  $V_s$  of MSW available in the literature. All three studies tested MSW from the Tri-Cities landfill (Zekkos et al. 2008; Lee 2007; Yuan et al. 2011). MSW samples from various locations were characterized according to the procedures described by Zekkos et al. (2010) and were separated into >20- and <20-mm waste fractions. The <20-mm fraction is typically soil-like in nature (i.e., includes significant amounts of daily cover soil and inorganic debris as well as fine waste inclusions). The >20-mm material consists primarily of waste generated at the source, i.e., primarily plastics, paper, and wood. Zekkos et al. (2008) performed cyclic triaxial tests on specimens with a diameter of 300 mm and nominal height of 600 mm. Lee (2007)

**Table 1.** Summary of Field Shear-Wave Measurements at MSW Landfills from the Literature and This Study

Landfill	Location	Number of soundings	Method	Reference
Azusa	California (United States)	6	SASW	Kavazanjian et al. (1996)
Lopez Canyon	California (United States)	4	SASW	Kavazanjian et al. (1996)
Toyon Canyon	California (United States)	1	SASW	Kavazanjian et al. (1996)
Sunshine Canyon	California (United States)	1	SASW	Kavazanjian et al. (1996)
Landfill A	California (United States)	2	SASW	Kavazanjian et al. (1996)
Operating Industries (OII)	California (United States)	27 <sup>a</sup>	SASW	Kavazanjian et al. (1996)
Villalba	Spain	1	SASW	Cuellar et al. (1998)
Bolton	Georgia (United States)	1	SASW	Rix et al. (1998)
Sanifill	Georgia (United States)	1	SASW	Rix et al. (1998)
Valdemingomez	Spain	1	SASW	Pereira et al. (2002)
Altamont	California (United States)	3	SASW	Lin et al. (2004)
Redwood	California (United States)	4	SASW	Lin et al. (2004)
Tri-Cities	California (United States)	7	SASW	Lin et al. (2004)
Olympic View Sanitary Landfill	Washington (United States)	3	SASW	Matasovic and Kavazanjian (2006)
Austin Community Landfill	Texas (United States)	1	SASW	Zalachoris (2010)
Oakland Heights	Michigan (United States)	3	MASW and MAM	This study
Arbor Hills	Michigan (United States)	4	MASW and MAM	This study
Sauk Trail Hills	Michigan (United States)	3	MASW and MAM	This study
Carleton Farms	Michigan (United States)	3	MASW and MAM	This study

Note: MAM = microtremor analysis method; MASW = multichannel analyses of surface waves; SASW = spectral analysis of surface waves.

<sup>a</sup>Mean and mean  $\pm$  SD profiles were only analyzed as reported by Kavazanjian et al. (1996).

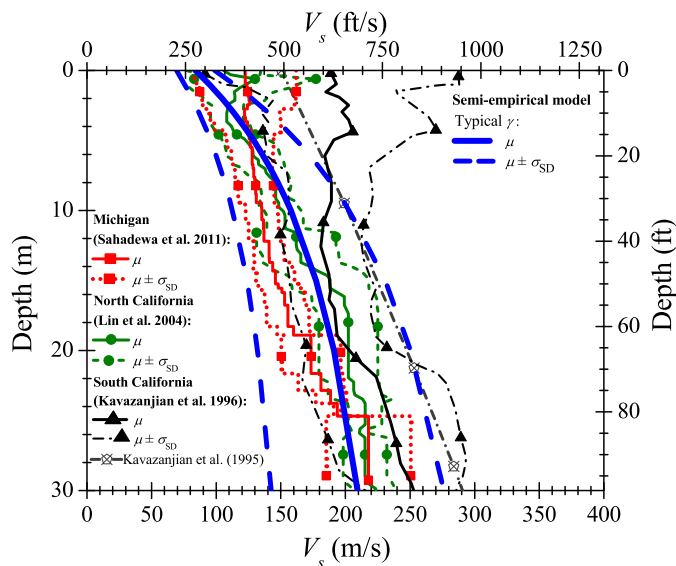


**Fig. 1.** Shear-wave velocity profiles at MSW landfills from the literature and this study

performed resonant column tests on specimens with a diameter of 150 mm and height of 300 mm. Yuan et al. (2011) performed 304- × 406-mm rectangular specimen cyclic simple shear tests at 75-kPa normal stress. Zekkos et al. (2008) and Lee (2007) also performed cyclic triaxial and resonant column tests, respectively, on conventional-sized specimens (71 mm in diameter) with only soil-sized (<20 mm) particles as well as with waste particles reduced to <20-mm size. The results showed that 71-mm-diameter specimens have different dynamic properties from those of the 300-mm-diameter MSW specimens. A concise discussion of the factors that affect the  $V_s$  of MSW is presented subsequently. A more extensive review of the linear and nonlinear dynamic properties of MSW has been presented by Zekkos et al. (2011).

### Confining Stress

Confining stress has a pronounced effect on  $V_s$  and  $G_{max}$ . Zekkos et al. (2008) reported increases in  $G_{max}$  by a factor of about 2 as the confining stress increases from 25 to 75 kPa. This represents a maximum increase in  $V_s$  by a factor of 1.4 (assuming no increase in density) according to Eq. (1). These data are consistent with the Lee (2007)  $V_s$  data from resonant column tests performed over a larger confining pressure range. Lee (2007) identified that at low confining pressures (<35–50 kPa), the waste is overconsolidated as a result of compaction and also showed that waste exhibits a significant effect of overconsolidation upon unloading. At the overconsolidated state, the influence of confining pressure on  $V_s$  and  $G_{max}$  is less significant; however, the values of  $V_s$  and  $G_{max}$  are larger than in the normally consolidated state (at the same confining pressure).

### Composition of MSW

The composition of MSW also significantly affects the  $V_s$ . Zekkos et al. (2008) reported a change in  $V_s$  from 80 to 150 m/s at a confining pressure of 75 kPa as the composition changes from waste-rich specimens (18% for <20-mm material by weight) to soil-rich specimens (100% for <20-mm material by weight). Yuan et al. (2011) also reported a change in  $V_s$  from approximately 75 to

140 m/s at a normal stress of 75 kPa as the composition changed from waste-rich specimens (35% for <20-mm material by weight) to soil-rich specimens (100% for <20-mm material by weight). Similarly, Lee (2007) found  $V_s$  to increase by a factor of 1.1–1.35 for changes in composition from 62–76 to 100% for <20 mm by weight at confining pressures up to 300 kPa. The somewhat smaller changes in  $V_s$  observed by Lee (2007) compared with Zekkos et al. (2008) may be a result of the smaller variation in waste composition in Lee's tests as well as the smaller sized particles. For the same compaction effort, as the waste composition changed, the unit weight of MSW also changed, with waste-rich specimens having lower unit weights. The data from Zekkos et al. (2008) suggest a strong correlation between  $V_s$  and the unit weight for all Tri-Cities waste specimens that had variable waste composition. Thus, as suggested in Zekkos et al. (2006), the unit weight of MSW can be considered an index of compactness as well as waste composition.

### Unit Weight

For reconstituted MSW specimens with identical waste composition, the unit weight (and the associated compaction effort) was found to have some impact on  $V_s$  and  $G_{max}$  (Zekkos et al. 2008). The  $G_{max}$  value increased by 10–20% from loosely compacted MSW specimens ( $\gamma_t = 10 \text{ kN/m}^3$ ) to densely compacted MSW specimens ( $\gamma_t = 12.5 \text{ kN/m}^3$ ) of the same composition tested at the same pressure. This effect is equivalent to an increase in  $V_s$  of MSW on the order of 3–7%, according to Eq. (1).

### Time under Confinement

The  $G_{max}$  value was found to increase significantly with time under confinement for the laboratory reconstituted specimens. The  $G_{max}$  value was found to double from 1 h under confinement to 1,000 h (about 40 days) under confinement (Zekkos et al. 2008). Lee (2007) also observed significant increases in  $V_s$  with time under confinement. Both studies indicated that the change in  $V_s$  is constant for every log cycle of time, similar to the behavior of uncemented natural soils.

### Loading Frequency

The loading frequency also has an impact on  $V_s$  and  $G_{max}$ , where the  $G_{max}$  value has increased by a factor of 1.1 per log cycle for frequencies ranging from 0.01 to 10 Hz (Zekkos et al. 2008). Lee (2007) independently showed similar results, and found that  $G_{max}$  increases by the same factor per log cycle of frequency for frequencies ranging from 0.03 to 260 Hz. The importance of the impact of frequency is that in situ seismic testing with borehole methods (e.g., crosshole) typically entails measurements at frequencies approaching 100–300 Hz, yielding higher estimates of  $V_s$  compared with surface wave methods where frequencies are in the 3–50 Hz range.

### Other Factors

The impact of a number of other factors on  $V_s$  and  $G_{max}$  of MSW remains unknown. The temperature in landfills is typically higher than ambient temperature because of the decomposition process. Landfill temperatures vary from 25 to 70°C (Hanson et al. 2010; Zekkos et al. 2010). The impact of increased temperature on the  $V_s$  value of MSW remains unknown. The impact of the previous cyclic stress history appears to be small based on Lee (2007); however, further studies are needed. Capillarity has been shown to play a role

in the  $V_s$  value of soils. Recent studies have focused on the characteristics of unsaturated MSW; however, the impact of moisture and capillarity on  $V_s$  of MSW has not been investigated. Finally, the impact of structural anisotropy as well as stress-induced anisotropy on  $V_s$  is largely unknown. MSW has been shown to be highly anisotropic in terms of shear resistance (Bray et al. 2009; Athanasopoulos et al. 2008), and this anisotropy should also impact  $V_s$ ; however, to a much lesser degree. In addition, stress-induced anisotropy has been shown to affect the propagation velocity of shear waves in soils (Bellotti et al. 1996; Stokoe and Santamarina 2000) and these factors will also impact  $V_s$  of MSW. In addition, the impact of waste decomposition on  $V_s$  remains unknown. More research is warranted to better understand these unresolved issues.

## Field Measurements of $V_s$ from This Study

### Procedure

Shear-wave velocity measurements were performed at four landfills in Michigan using a surface wave-based methodology that combines active and passive methods to develop a dispersion curve. Tests were performed at 13 locations at these landfills and the results are presented in more detail in Sahadewa et al. (2011).

The implemented methodology combined the active MASW method with the passive microtremor analysis method (MAM). The benefit of combining methods was the ability to overlap the dispersion curves of surface waves that have higher frequencies of excitation with the lower frequencies associated with passive techniques and extend the frequency content of the collected data. This allowed an independent comparison between the methods and the ability to transition from shorter to longer wavelengths with increased confidence in the collected data. The MASW measurements typically provided information at higher frequencies (shorter wavelengths) in the range of 4.5–30 Hz, whereas the MAM measurements provided data at lower frequencies (longer wavelengths) in the range of 2.5–8 Hz, depending on the frequency content of the background noise. As such, the MAM was valuable in collecting information at greater depths and broadening the frequency range of the dispersion curve.

For this investigation, a linear array consisting of sixteen 4.5-Hz geophones with 3-m spacing between geophones was used. The resulting total spread length was 45 m. The geophone spacing was selected to prevent spatial aliasing, maintain a high signal-to-noise ratio, and result in a total spread length that will maximize the depth of investigation.

For the MASW (active) measurements, a 44-N sledge hammer was typically used as the source, allowing for assessment of the  $V_s$  profile to a depth of 15–20 m. The source impacts were located 4.5 m from the first geophone of the array. Signal stacking permitted increased signal-to-noise ratio. In general, depending on the background noise level, between five and eight repetitions were stacked to generate one MASW record. In some cases, landfill construction vehicles were also used to generate vibrations, similar to active sources used by Lin et al. (2004) in SASW testing.

For the MAM (passive) measurements, a circular, hexagonal, triangular, or L-shaped geometric configuration is recommended (e.g., Park et al. 2004; Asten et al. 2004) to ensure that the results are not impacted by the directivity of the background noise. More recently, research was conducted to evaluate the reliability of the passive methodology using a linear array (e.g., Tran and Hiltunen 2008; Cox and Beekman 2011; Strobbia and Cassiani 2011). In this investigation, MAM data were collected for field testing efficiency purposes using the same linear geophone configuration previously

described for the MASW tests. Efforts were made to identify the dominant sources of noise, which in landfills can be often readily done (Sahadewa et al. 2012). Twenty recordings in total, each lasting 32 s, were collected to capture surface waves generated by cultural activities (e.g., traffic and construction activities) and other sources at each testing location.

The active and passive measurements were separately transformed into active and passive dispersion curves, respectively, which showed the variation of propagation velocity (i.e., phase velocity  $V_{ph}$ ) with frequency of Rayleigh waves. In this process, undesirable waves in the MASW and MAM tests, such as body waves, higher-mode Rayleigh waves, and other noise were identified. For normally dispersive sites (i.e., sites where  $V_{ph}$  increases with depth), the fundamental mode dispersion curve of the Rayleigh wave was extracted. For inversely dispersive sites, where a high-velocity layer overlays a lower-velocity layer, higher modes of Rayleigh waves were considered in the analysis (Tokimatsu et al. 1992). The MASW and MAM records were transformed to a dispersion curve using various signal processing methodologies. The Park et al. (1999b) procedure was implemented for the development of the dispersion curve from the MASW (active) data. In the MAM, the 20 recordings at each location were transformed to a passive dispersion curve using the spatial autocorrelation (SPAC) method (Aki 1957; Okada 2003). Because the SPAC method assumes that the background vibrations are omnidirectional, the MAM data generated using the linear array may prove to be unreliable (Sahadewa et al. 2012). When this problem became apparent during the data analyses, the passive MAM data were not used.

Examples of the dispersion curves derived from MASW and MAM at one location at the Sauk Trail Hills landfill are presented in Fig. 2. Additional examples of the MASW and MAM combined dispersion curves are presented in Sahadewa et al. (2011). The independently developed dispersion curves from the MASW and MAM data were then compared. In this case, for frequencies between 5 and 7 Hz, the dispersion data from the active and passive measurements overlapped quite well. In cases, such as shown in Fig. 2, where the passive dispersion curve agreed well with the active dispersion curve, the MAM provided additional information for frequencies down to 2.5 Hz that were not available in the active data. In other cases, the MAM data did not agree with the MASW data and the phase velocities estimated using the MAM were higher than those estimated by the MASW method. This discrepancy is likely attributable to the method of analysis (SPAC method) and the use of a linear array with complicating directionality in background noise. A linear array of geophones will not satisfy the omnidirectionality assumption when a dominating passive signal originates from one direction. Depending on the orientation of the array, the results may be unreliable (Sahadewa et al. 2012). When the active and passive dispersion curves did not agree, the dispersion curves derived from only the active data were used in the forward modeling process because the surface wave source was well defined in this case. Fig. 3 shows the complete dispersion curve for Location 1 at the Sauk Trail Hills landfill site derived from the active and passive data of Fig. 2.

In the forward modeling process, an assumed  $V_s$  profile was back-calculated to obtain a theoretical dispersion curve assuming a Poisson's ratio of 0.2 for MSW. The theoretical curve was compared against the measured dispersion curve, and changes in the assumed model were made iteratively until the two curves matched closely. A nonlinear least-squares method was implemented to evaluate matching (Xia et al. 1999).

The layering resolution for all surface wave-based methodologies reduces with depth (Gucunski and Woods 1992). Thinner layers can be more easily discerned near the surface than at the depth. At greater depths, only thicker layers can be clearly identified and the

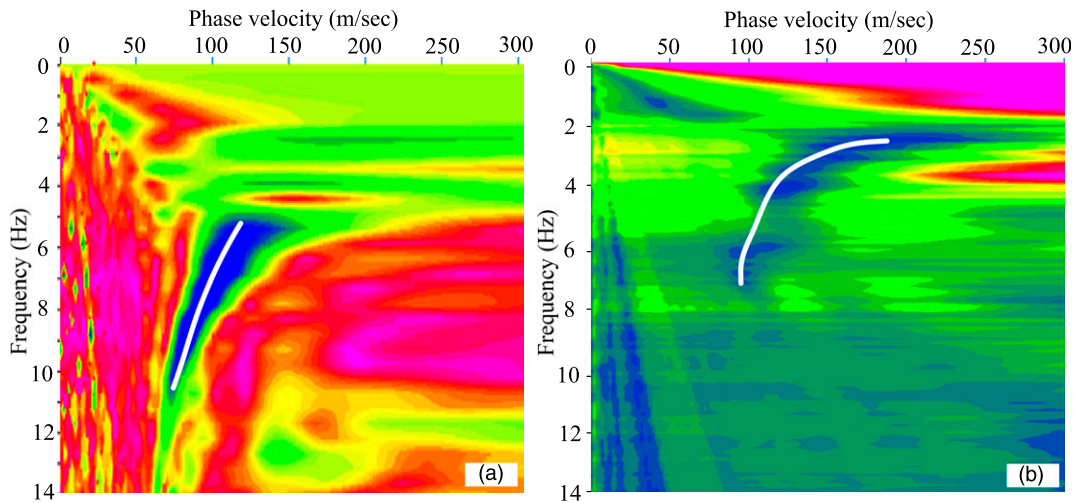


Fig. 2. Dispersion curve analyses of (a) MASW and (b) MAM data at Location 1 at the Sauk Trail Hills landfill

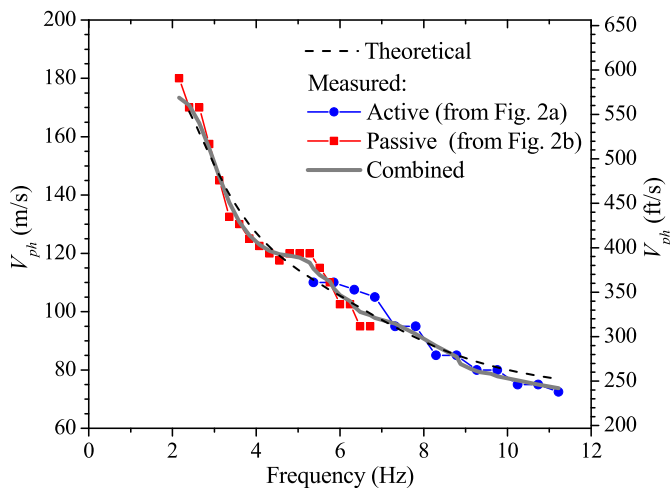


Fig. 3. Field dispersion curves determined from a combination of active and passive dispersion curves at Sauk Trail Hills 1 shown in Fig. 2

estimated phase velocity represents an estimate of the  $V_s$  of the subsurface that is averaged. This resolution issue is a limitation of surface wave-based methodologies; however, surface waves caused by earthquakes also do not sense such thin layers because of their long wavelengths.

### Results of Field Measurements

The thirteen  $V_s$  profiles at the Arbor Hills, Oakland Heights, Carleton Farms, and Sauk Trail Hills landfills in southeast Michigan are presented in Fig. 4. Of the 13  $V_s$  profiles, six were derived using only the MASW data (i.e., Arbor Hills 1 and 2, Oakland Heights 1 and 2, Sauk Trail Hills 2, and Carleton Farms 2) and the remaining seven were derived using the combined MASW and MAM data. Generally,  $V_s$  of MSW at these landfills is increasing with depth, with values ranging from about 70 m/s at the surface to 200 m/s at a depth of about 25 m. In several cases, a higher  $V_s$  layer with a thickness of as much as 5 m was identified near the surface. Landfill data and exploration pits confirmed that these higher  $V_s$  layers were not MSW but contaminated soils or fills placed to allow access to traffic. In two landfill locations, light-weight auto fluff material was

used instead of daily soil cover. The auto fluff consisted of non-metallic shredded pieces of vehicles; typically, soft and stiff plastics, foam, and other parts of the interior of vehicles. In these locations, the lowest  $V_s$  values ( $\leq 80$  m/s) were observed (e.g., Carleton Farms Location 2 and Sauk Trail Hills Location 1). Information about these Michigan landfills, the results of the field measurements, as well as the associated dispersion curves are presented in more detail in Sahadewa et al. (2011).

### Models for $V_s$ and $G_{\max}$ of MSW

The  $V_s$  and associated  $G_{\max}$  of soils have been studied extensively for many years (e.g., Hardin and Drnevich 1972; Seed and Idriss 1970; Richart 1975; Hardin 1978; Kokusho et al. 1982; Dobry and Vucetic 1987; Stokoe and Santamarina 2000; Menq 2003; among others). The generic forms of the equations describing  $V_s$  and  $G_{\max}$  are

$$V_s = A_{V_s} \cdot p(e) \cdot \sigma'_o{}^r \quad (2a)$$

$$G_{\max} = A_G \cdot f(e) \cdot \sigma'_o{}^m \quad (2b)$$

where  $A_G$  and  $A_{V_s}$  = material parameters affected by various factors such as soil type, overconsolidation ratio, strain rate, and other factors;  $f(e)$  and  $p(e)$  = mathematical functions describing the effect of void ratio ( $e$ ) on  $G_{\max}$  and  $V_s$ , respectively;  $\sigma'_o$  = effective confining stress; and finally,  $m$  and  $r$  = exponents of confining stress, with  $r = m/2$ . Most commonly,  $\sigma'_o$  represents the isotropic confining stress because specimens in laboratory dynamic testing equipment (such as torsional resonant columns) are subjected to an isotropic stress state. Subsequent studies have shown that an anisotropic stress state, either in the laboratory or in the field, induces anisotropy in wave propagation velocities (Bellotti et al. 1996; Stokoe et al. 1991). In Eq. (2b),  $G_{\max}$  is related to the isotropic stress by a power function with a stress exponent  $m$ . Many studies have shown that this exponent is usually in the range of 0.45–0.65, with small variations reported for different soils (Hardin and Richart 1963; Hardin and Black 1968; Iwasaki and Tatsuoka 1977; Hryciw and Thomann 1993; Zhou and Chen 2005).

Two models were developed for  $V_s$  of MSW. The first model is a semiempirical model and the second model is an empirical model.

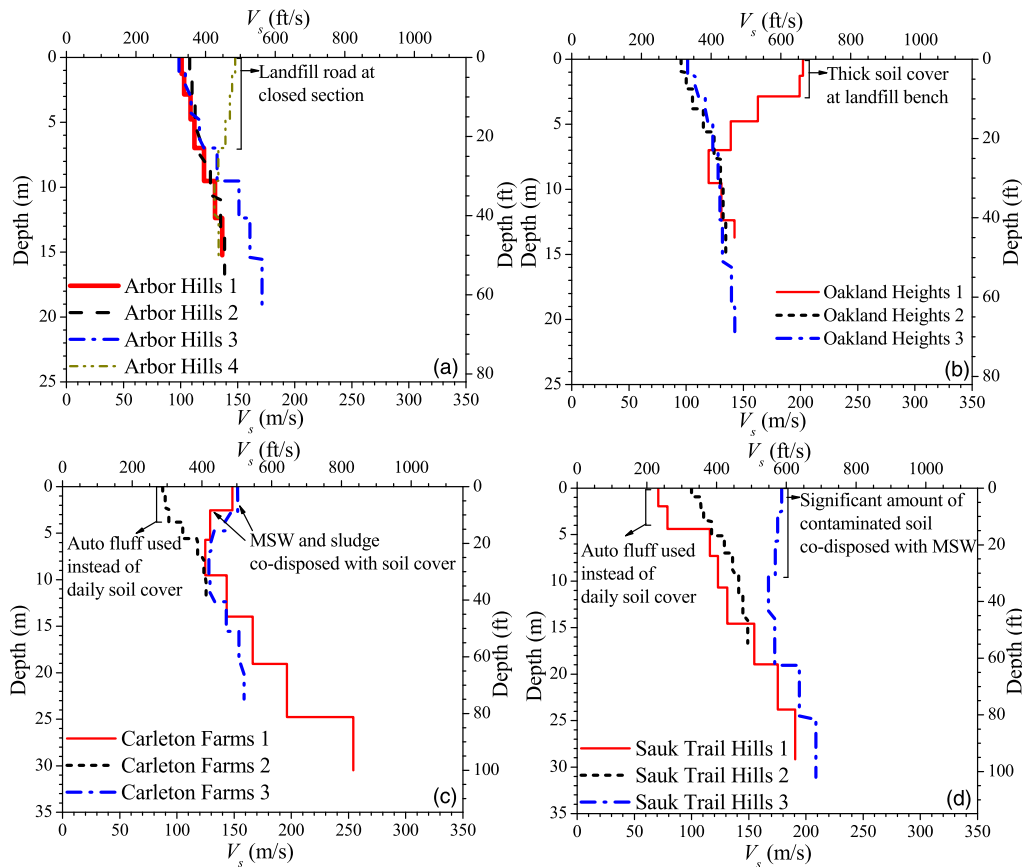


**Fig. 4.** Shear-wave velocity measurements at (a) Arbor Hills landfill; (b) Oakland Heights landfill; (c) Carleton Farms landfill; (d) Sauk Trail Hills landfill

A brief description of each model is provided. Then, the formulation and the calibration of the two models are presented.

### Semiempirical Model for $V_s$ of MSW

The semiempirical model for  $G_{\max}$  and  $V_s$  of MSW is consistent with models developed for soils. The semiempirical model is a comprehensive model that aims to separate the influence of waste density (and by extension, waste composition) and confining stress on the  $V_s$  of MSW. As such, it involves more variables and its mathematical expression is more complex. Similar to the models developed for soils [Eqs. (2a) and (2b)], the model is mathematically formulated on the basis of laboratory experimental data. Once the mathematical expression is derived it is used to match field data, and the model's parameters are calibrated. Thus, the development of the semiempirical model requires two phases and is more laborious compared with the empirical model.

### Empirical Model for $V_s$ of MSW

The empirical model is a mathematically simpler model that relates the shear-wave velocity to the depth. It is calibrated simply by fitting it to the field measurements of the  $V_s$  of MSW and empirically deriving the model parameters. As long as the model's mathematical function can fit the data, its expression is not as critical because its formulation is not intended to describe material behavior. As a consequence, the empirical model does not capture the influence of the various factors on  $V_s$  that have been shown in the laboratory to affect it. Instead, the influence of these factors contributes to the variance of the model parameters.

### Formulation of the Semiempirical Model from Laboratory Data

The generic form of the  $V_s$  model is

$$V_s = g\left(\frac{\gamma_t}{\gamma_w}\right) \cdot h\left(\frac{\sigma'_o}{P_a}\right) \quad (3)$$

where  $g(\gamma_t)$  = function describing the relationship of  $V_s$  to the total unit weight of the MSW; and  $h(\sigma'_o)$  = function describing the relationship of  $V_s$  with the effective isotropic confining stress. An equivalent equation can be derived for  $G_{\max}$  because  $G_{\max}$  and  $V_s$  are related through Eq. (1). In formulating the relationship, the functions were normalized by the unit weight of water ( $\gamma_w$ ) and atmospheric pressure ( $P_a$ ), respectively. As shown in Eq. (2), previous equations for soils have used the void ratio or relative density to describe the compactness of soils. Both are impractical to apply to MSW. Thus, the total unit weight is used instead. The unit weight, briefly discussed previously and described in more detail in Zekkos et al. (2006), is an indicator of waste compactness and waste composition. For the same depth (or confining pressure), lower unit weights are correlated with waste-rich MSW, and higher unit weights are correlated with soil-rich MSW. Thus, the  $g(\gamma)$  function also indirectly captures variations in waste composition.

The data from large-scale laboratory specimens generated by Zekkos et al. (2008) and Lee (2007) were used to derive the mathematical form of Eq. (3). Lee (2007) measured  $V_s$  of the MSW specimens. The Zekkos et al. (2008) data were generated from cyclic triaxial testing that involved measurement of the modulus. Because

$G_{max}$  and  $V_s$  are related through Eq. (1) and the density of the specimens is always known, once either  $G_{max}$  or  $V_s$  is measured, the other parameter can be calculated. Fig. 5(a) shows the Zekkos et al. (2008)  $G_{max}$  data for MSW triaxial specimens at a confining stress of 75 kPa and at 24-h time under isotropic confinement. The data set includes all specimens from various waste samples (A3, C3, and C6) (as described by Zekkos et al. 2008) tested at this confining stress level. The data set includes specimens that consisted entirely of <20-mm material, specimens of intermediate (and more typical) waste composition (62–76% for <20 mm by weight), and specimens that consisted almost entirely of the coarse waste fraction (17% for <20 mm by weight). A generic relationship between the unit weight and  $G_{max}$  [Fig. 5(a)] or  $V_s$  [Fig. 5(b)] was derived for all MSW specimens from this study with a high coefficient of determination ( $R^2$ ). These relationships are described by the following equations:

$$G_{max} = B_G \left( \frac{\gamma_t}{\gamma_w} \right)^{n_\gamma} \quad \text{at } \sigma'_o = \text{constant} \quad (4a)$$

$$V_s = B_{V_s} \left( \frac{\gamma_t}{\gamma_w} \right)^{r_\gamma} \quad \text{at } \sigma'_o = \text{constant} \quad (4b)$$

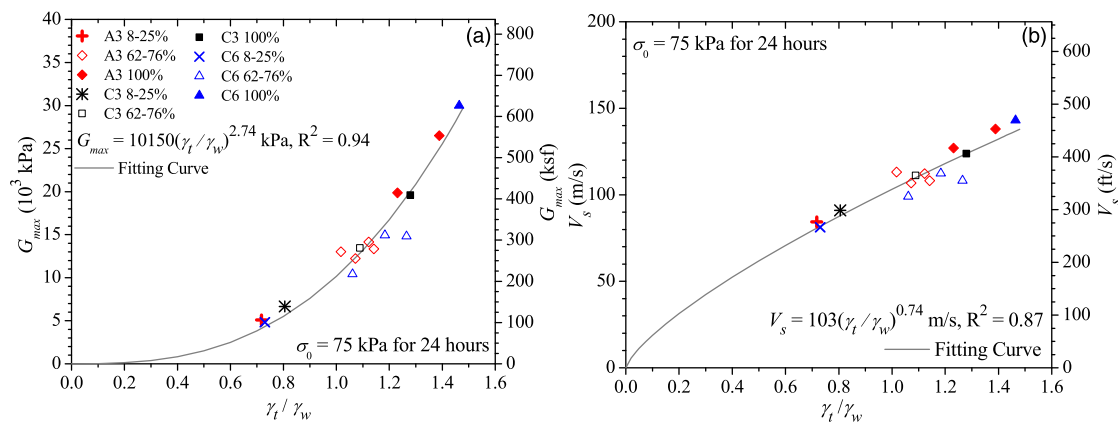


**Fig. 5.** Relationship between (a)  $G_{max}$  or (b)  $V_s$  and the normalized total unit weight of MSW from the Zekkos et al. (2008) laboratory data for testing at  $\sigma_o = 75$  kPa and 24 h under confinement

As shown subsequently,  $B_G$  and  $B_{V_s}$  are not constants but are variables that are a function of the confining stress. Based on regression analyses, for the Zekkos et al. (2008) data,  $B_G$  is equal to 10,150 kPa and  $n_\gamma$  is equal to 2.74, with a coefficient of determination of 0.94 for measurements at  $\sigma'_o = 75$  kPa. Similarly,  $B_{V_s}$  is equal to 103 m/s and  $r_\gamma$  is equal to 0.74, with a coefficient of determination of 0.87. Analyses were also performed for the Lee (2007) data set that included tests performed at confining stresses varying from 8 to 276 kPa, and the results are shown in Figs. 6(a and b). The resulting  $B_G$ ,  $B_{V_s}$ ,  $n_\gamma$ , and  $r_\gamma$  values for the Lee (2007) and Zekkos et al. (2008) data are presented in Table 2 along with associated  $R^2$  coefficients. The scatter in the Lee (2007) data are somewhat higher than in the Zekkos et al. (2008) data, partly because the Lee (2007) data were not collected at the same time under confinement (24–48 h at each confining pressure level), as was the case for the Zekkos et al. (2008) data (24 h).

The value of the  $n_\gamma$  parameter varied from 1.7 to 2.0 for the Lee (2007) data. Most of the data appear to indicate a small reduction of the  $n_\gamma$  parameter with confining stress, although the value of  $n_\gamma$  at a confining stress level of 276 kPa is high. Regardless, a variation between 1.7 and 2.0 is not significant for practical purposes. The  $n_\gamma$  parameter takes a higher value ( $n_\gamma = 2.74$ ) for the Zekkos et al.

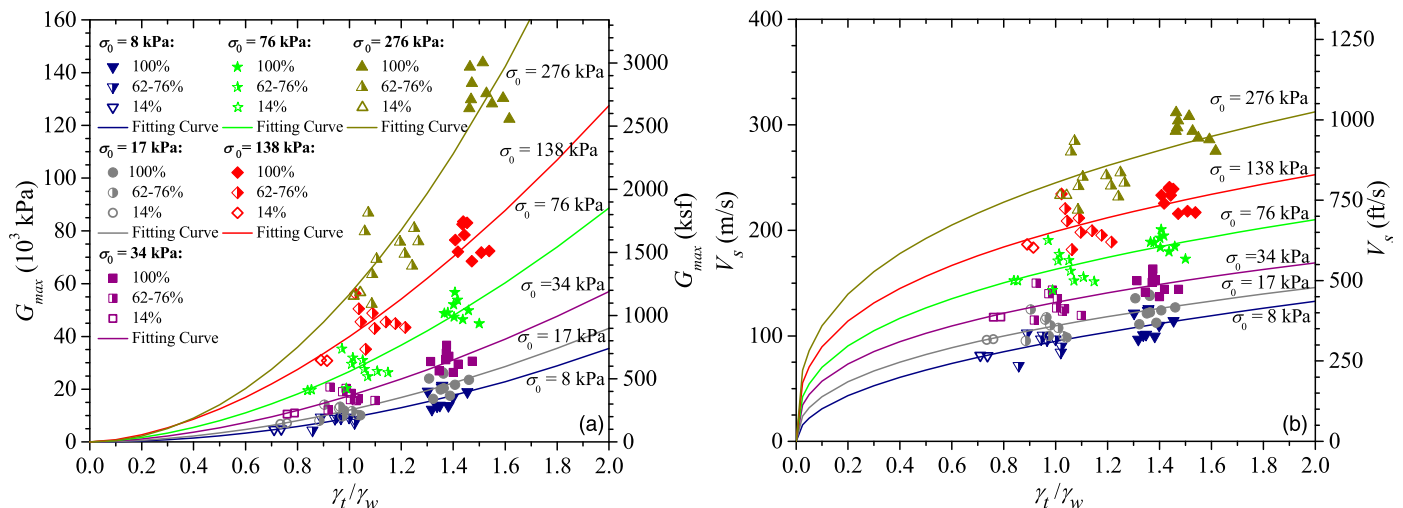


**Fig. 6.** Relationship between (a)  $G_{max}$  or (b)  $V_s$  and the normalized total unit weight of MSW from the Lee (2007) laboratory data (percentages indicate the percent of <20-mm material)

(2008) data at a confining stress of 75 kPa. The differences in the  $B_G$  and  $n_\gamma$  values for the Zekkos et al. (2008) and the Lee (2007) data may be attributed to several differences in the testing variables. Some of these differences may include variations in testing frequency, time under confinement, specimen size [i.e., a diameter of 300 mm for the Zekkos et al. (2008) data and a diameter of 150 mm for the Lee (2007) data], particle size, specimen preparation, and compaction methods, and possibly the type of testing apparatus [i.e., cyclic triaxial testing for Zekkos et al. (2008) versus resonant column testing for Lee (2007)]. However, waste variability is probably not a contributor to this variability because the source of the waste material was the same in the two studies. Although the values of the  $n_\gamma$  parameter for the Lee (2007) data are lower, they also fit the Zekkos et al. (2008) data with high coefficients of determination.

Using the Lee (2007) laboratory data, the relationships between  $B_G$ ,  $B_{V_s}$ , and the confining stress were established and are shown in Figs. 7(a and b). The  $B_G$  and  $B_{V_s}$  values generally increase with confining stress. A power function was first used for the regression analyses because this function has been commonly used for soils (in kilopascals)

$$B_G = 32,580 \left( \frac{\sigma'_o}{P_a} \right)^{0.55} \quad (5)$$

The regressed stress exponent was found to be equal to 0.55, which is within the range recommended for soils (e.g., Hardin and Richart 1963; Hardin and Black 1968).

**Table 2.** Regressed  $B_G$ ,  $B_{V_s}$ ,  $n_\gamma$ , and  $r_\gamma$  Values and Associated  $R^2$  Coefficients for the Lee (2007) and Zekkos et al. (2008) Laboratory Data Sets

Data set	$\sigma_0$ (kPa)	$B_G$ (kPa)	$n_\gamma$	$R^2$	$B_{V_s}$ (m/s)	$r_\gamma$	$R^2$
Lee (2007)	8	9,080	1.97	0.79	95	0.49	0.55
	17	12,080	1.83	0.81	110	0.41	0.51
	34	17,500	1.70	0.84	132	0.36	0.50
	76	26,750	1.73	0.84	163	0.37	0.46
	138	39,930	1.67	0.82	199	0.35	0.43
	276	55,950	1.99	0.84	245	0.35	0.50
Zekkos et al. (2008)	75	10,150	2.74	0.94	103	0.74	0.87

A hyperbolic function has also been used for soils and is also used here for the regression analysis. Although both the power and hyperbolic functions closely fit the data with very high  $R^2$  values ( $R^2 = 0.999$ ), the power function indicates that the  $B_G$  parameter (and by extension  $G_{max}$  and  $V_s$ ) results in a zero value at zero confining stress. Zero effective stiffness at zero confining stress (e.g., at the landfill surface) is not a realistic assumption. For MSW in particular, the waste has variable waste constituents, particles with large sizes in at least one or two directions, and capillary stresses. The hyperbolic function accommodates that aspect of finite stiffness of the MSW at the landfill surface. Regression analyses of the Lee (2007) data indicate the following equations for the hyperbolic functions:

$$B_G = 6,390 + \frac{101,500 \times (\sigma'_o/P_a)}{2.8 + (\sigma'_o/P_a)} \quad (6a)$$

$$B_{V_s} = 83 + \frac{224 \times (\sigma'_o/P_a)}{1.3 + (\sigma'_o/P_a)} \quad (6b)$$

In these equations, parameter  $B_G$  is in kilopascals and  $B_{V_s}$  is in meters per second. The laboratory-based values for the  $B$  parameters are not as critical because they are representative of reconstituted laboratory specimens that have been under isotropic confining stress for a relatively short amount of time. However, the mathematical expression of the equation derived from the laboratory data should capture the relationship of  $G_{max}$  and  $V_s$  with the unit weight and effective confining stress in the field and can be used to calibrate the relationship against field data.

### Calibration of $V_s$ Models against Field Data

#### Semiempirical Model

Based on the laboratory data, the mathematical expression of the semiempirical  $V_s$  equation is as follows:

$$V_s = \left[ A_L + \frac{B_L \times (\sigma'_o/P_a)}{C_L + (\sigma'_o/P_a)} \right] \left( \frac{\gamma_t}{\gamma_w} \right)^{r_\gamma} \quad (7)$$

Eq. (7) is a function of isotropic effective confining stress  $\sigma'_o$  and MSW total unit weight  $\gamma_t$ . The parameters  $A_L$ ,  $B_L$ ,  $C_L$ , and  $r_\gamma$  are

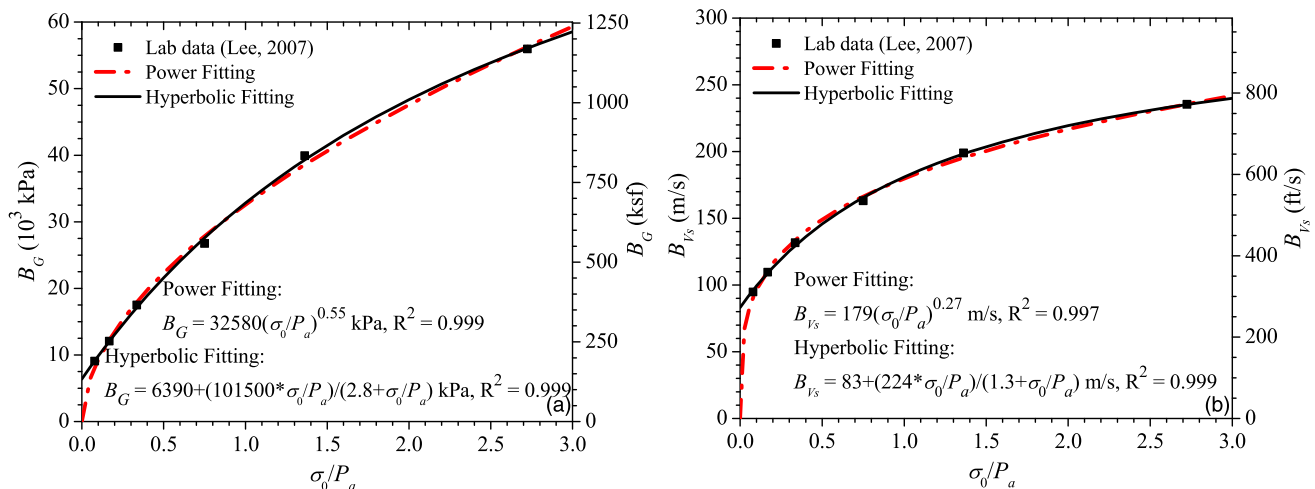


**Fig. 7.** Relationship between the (a)  $B_G$  or (b)  $B_{V_s}$  function and the normalized isotropic confining stress based on the laboratory data from Lee (2007)

model fitting parameters based on the laboratory data. The  $A_L$  parameter is directly related to the value of  $V_s$  at zero confining stress. Low  $A_L$  values are indicative of low  $V_s$  at zero effective confining stress (or at the surface of the landfill). High  $A_L$  values are indicative of high  $V_s$  at zero effective confining stress. The  $B_L$  and  $C_L$  parameters are both directly related to the rate of increase of  $V_s$  with confining stress. A similar expression of this equation for field conditions can be formulated as

$$V_s = \left[ A_F + \frac{B_F \times (\sigma'_v/P_a)}{C_F + (\sigma'_v/P_a)} \right] \left( \frac{\gamma_t}{\gamma_w} \right)^{r_\gamma} \quad (8)$$

Eq. (8) is also a function of the effective confining stress and MSW total unit weight; however, in the field MSW is under anisotropic stress conditions. Because of uncertainties associated with calculating the lateral earth pressure at the rest coefficient,  $K_0$ , for MSW (Zekkos 2005), it is more convenient to formulate the model as a function of the vertical effective stress. In this case, parameters  $A_F$ ,  $B_F$ ,  $C_F$ , and  $r_\gamma$  are model fitting parameters based on the field data. The vertical effective stress is equal to the product of the effective unit weight of MSW and depth. For dry tomb landfills (such as Subtitle D landfills) that are designed to minimize the introduction of liquids into the waste mass, the waste remains unsaturated. Thus, the effective stress may be higher than the total stress as a result of capillary stresses, and if capillary stresses are insignificant the total stress and effective stress are equal. In this formulation capillary stresses are ignored, and thus if the waste is unsaturated the effective and total stresses are the same. This is a necessary assumption because capillary stresses in the unsaturated regime for a multisize, multiconstituent material, such as MSW, are unknown.

The total unit weight of the MSW needs to be estimated (or measured, if practical) to estimate  $V_s$  using the semiempirical equation [Eq. (8)]. Zekkos et al. (2006) described the procedures to perform in situ unit weight measurements. Alternatively, a hyperbolic model for the unit weight of MSW was proposed. The unit weight was found to be affected by the compaction effort and composition as well as the confining stress and is estimated by the following equation:

$$\gamma_t = \gamma_i + \frac{z}{\alpha + \beta \cdot z} \quad (9)$$

where  $\gamma_i$  = in-place total unit weight at the surface ( $\text{kN/m}^3$ );  $z$  = depth at which the MSW unit weight  $\gamma_t$  is to be estimated (m); and  $\alpha$  and  $\beta$  = modeling parameters ( $\text{m}^4/\text{kN}$  and  $\text{m}^3/\text{kN}$ , respectively). Calibration of the model using field test data yielded values for  $\gamma_i$ ,  $\alpha$ , and  $\beta$  that are a function of the compaction effort and amount of soil-like material (particle size  $<20$  mm) and are given in Table 3. Use of Eq. (9) in Eq. (8) allows the formulation of a model for  $V_s$  that is only a function of depth  $z$ ; however, this mathematical expression is more complex.

To simplify the regression analyses,  $C_F$  was set equal to 1.3 based on the value determined from the Lee (2007) and Zekkos et al. (2008) laboratory data. Although the value of  $C_F$  could also be

**Table 3.** Hyperbolic Parameters for Various Compaction Efforts and Amounts of Soil Cover (as Recommended by Zekkos et al. 2006)

Compaction effort and soil amount	$\gamma_i$ ( $\text{kN/m}^3$ )	$\beta$ ( $\text{m}^3/\text{kN}$ )	$\alpha$ ( $\text{m}^4/\text{kN}$ )
Low	5	0.1	2
Typical	10	0.2	3
High	15.5	0.9	6

calibrated against the field data, this was not deemed necessary because  $C_F$  does not vary significantly and calibrating the  $B_F$  parameter has a similar effect on the model. The Lee (2007) laboratory data suggest  $r_\gamma$  values between 0.35 and 0.50 for a range of confining stresses. The larger size triaxial data by Zekkos et al. (2008) at a confining stress of 75 kPa indicate a value of 0.74. The model was calibrated using values of 0.5 and 0.6. The  $r_\gamma$  value of 0.6 was found to result in smaller variability in the  $B_F$  field-calibrated values. Because this value also evenly weighs the available laboratory data sets,  $r_\gamma$  equal to 0.6 was used for the subsequent model regressions.

The model was calibrated against 36 soundings at 15 landfills available in the literature, as well as the 13 soundings at four landfills generated as part of this study (Table 1). For the OII landfill, the model was calibrated against the mean ( $\mu$ )  $V_s$  profile as well as the mean plus or minus one SD ( $\mu \pm \sigma_{SD}$ )  $V_s$  profiles of the set of 27  $V_s$  profiles. For the Lopez Canyon landfill, the mean  $V_s$  profile was used in the calibration process. As part of the calibration process, the model was fitted as closely as possible to each sounding and the values for parameters  $A_F$  and  $B_F$  were derived. Model fits to each  $V_s$  profile were not made using a least-squares or other regression scheme but were made visually such that the overall shape of the modeled profile followed the measured  $V_s$  profile.

For the semiempirical model for  $V_s$  [Eq. (8)], a unit weight variation with depth for each landfill in the database is needed for calibrations. For three landfills (OII, Azusa, and Tri-Cities) the available in situ unit weight data (Zekkos et al. 2006) were used for the calibrations. For the remaining landfills, the recommendations by Zekkos et al. (2006) were followed to select a representative unit weight profile. Through that process the typical unit weight profile was used for 27 soundings, and the high unit weight profile was used for six soundings only.

### Empirical Model

As discussed earlier, alternatively, a purely empirical model for the variation of  $V_s$  with depth can be used. A hyperbolic form was used for the model because this mathematical expression facilitates fitting  $V_s$  versus depth profiles of various curvatures. The empirical model used is

$$V_s = V_{si} + \frac{z}{\alpha_{V_s} + \beta_{V_s} \times z} \quad (10)$$

where  $V_{si}$  = estimated shear-wave velocity at the surface (without considering the presence of any crust); and  $\alpha_{V_s}$  and  $\beta_{V_s}$  = hyperbolic model fit parameters. As shown in Eq. (10), the main advantage of the empirical model compared with the semiempirical model is that it does not require an estimate of the MSW unit weight.

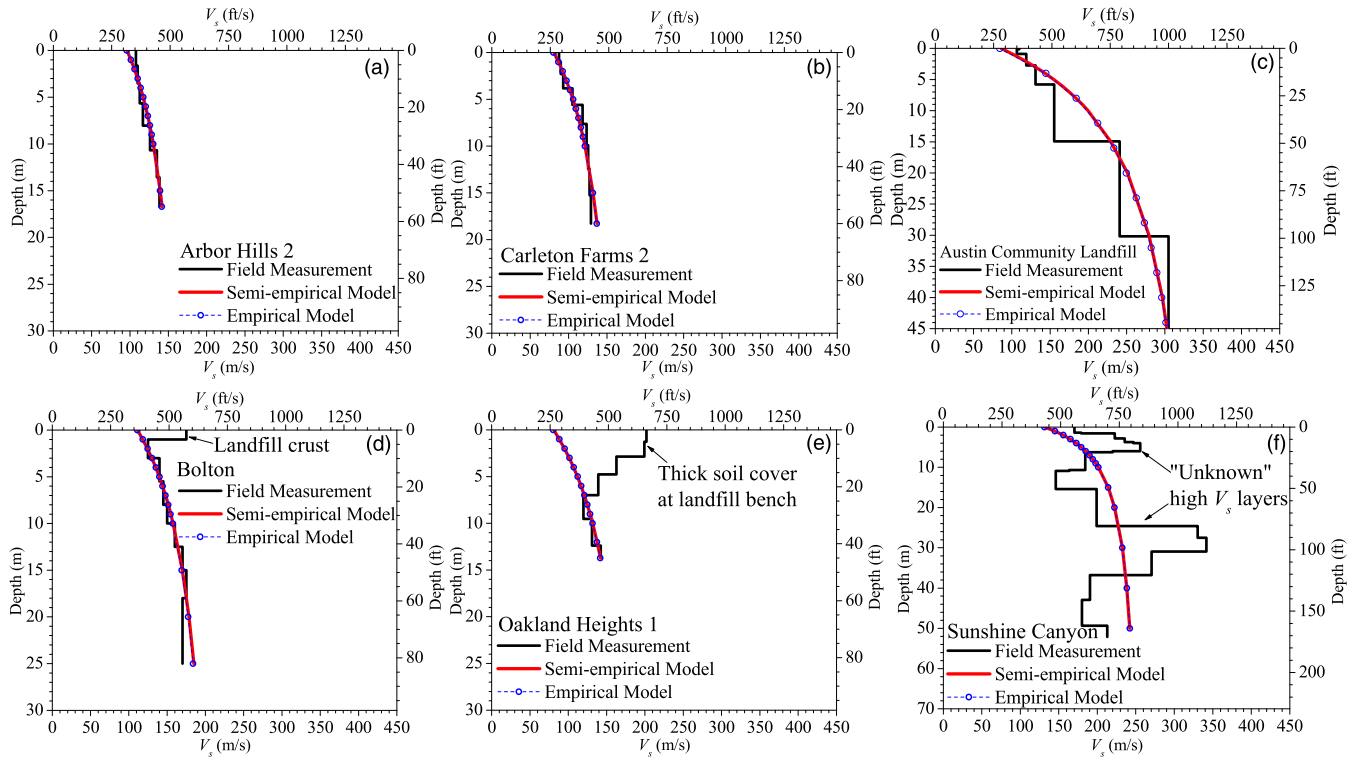
### Field Calibration Results for Semiempirical and Empirical Models

Fig. 8 shows examples of the calibrations of both models [Eq. (8) for the semiempirical and Eq. (10) for the empirical] against the field  $V_s$  data at various landfills from the literature and this study. The calibrations were used to derive the semiempirical ( $A_F$  and  $B_F$ ) and empirical ( $V_{si}$ ,  $\alpha_{V_s}$ , and  $\beta_{V_s}$ ) parameters for each site. For most locations (27 out of 49),  $V_s$  increases with depth, and the models nicely capture this behavior. Examples of such locations are shown in Figs. 8(a–c). At some locations (15 out of 49), such as those shown in Fig. 8(d), a layer of higher  $V_s$  (or landfill crust) is observed at the surface, with  $V_s$  values of 150–250 m/s. This layer is typically the result of a compacted daily soil cover, or a final composite cover, and has varying thicknesses that may reach 3–4 m (Matasovic and Kavazanjian 2006; Rix et al. 1998). In a few locations (seven out of 49), such as those shown in Figs. 8(e and f),

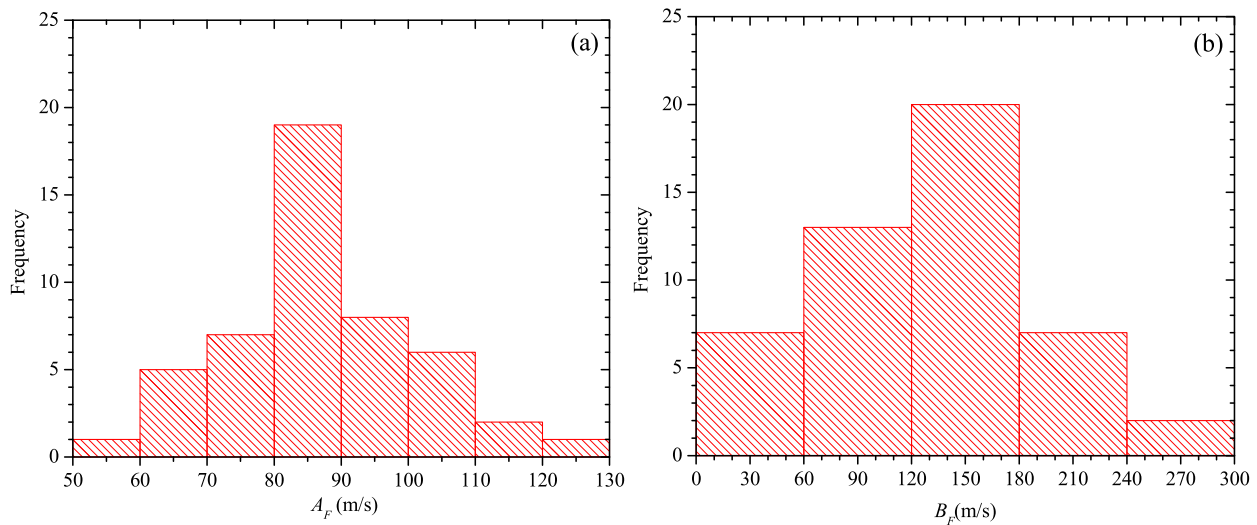
a high  $V_s$  layer is identified near the surface or at some depth underlain by the lower  $V_s$  layers at the depths below. For example, in the case of Oakland Heights 1 [Fig. 8(e)], as confirmed by trial test pits, a significant amount of soil cover was used to construct a landfill bench that is accessible to traffic. The reason for the high  $V_s$  layer at a depth of 30 m in Sunshine Canyon is unknown to the authors [Fig. 8 (f)]. Such irregularities may be attributed to major changes in waste composition, and possibly the presence of various waste materials, such as construction and demolition debris. The presence of these layers can create significant challenges in data interpretation during the application of simplified surface wave-based methodologies.

The proposed model is not suited to capturing such irregularities, which can only be typically verified via site-specific in situ measurements with boreholes or some other type of penetration testing.

Figs. 9(a and b) illustrate the results of the calibration of the semiempirical model against the field data in terms of the  $A_F$  and  $B_F$  parameters. The statistical analysis of the calibrated parameters indicates that the  $A_F$  and  $B_F$  parameters have normal distributions with a pronounced mode. Table 4 shows the  $\mu$ ,  $\sigma_{SD}$ , and other statistics of these parameters. The  $A_F$  and  $B_F$  parameters are not independent but are weakly negatively correlated, as shown in Fig. 10 and indicated in Table 4 by the low  $R^2$  value ( $R^2 = 0.48$ ).



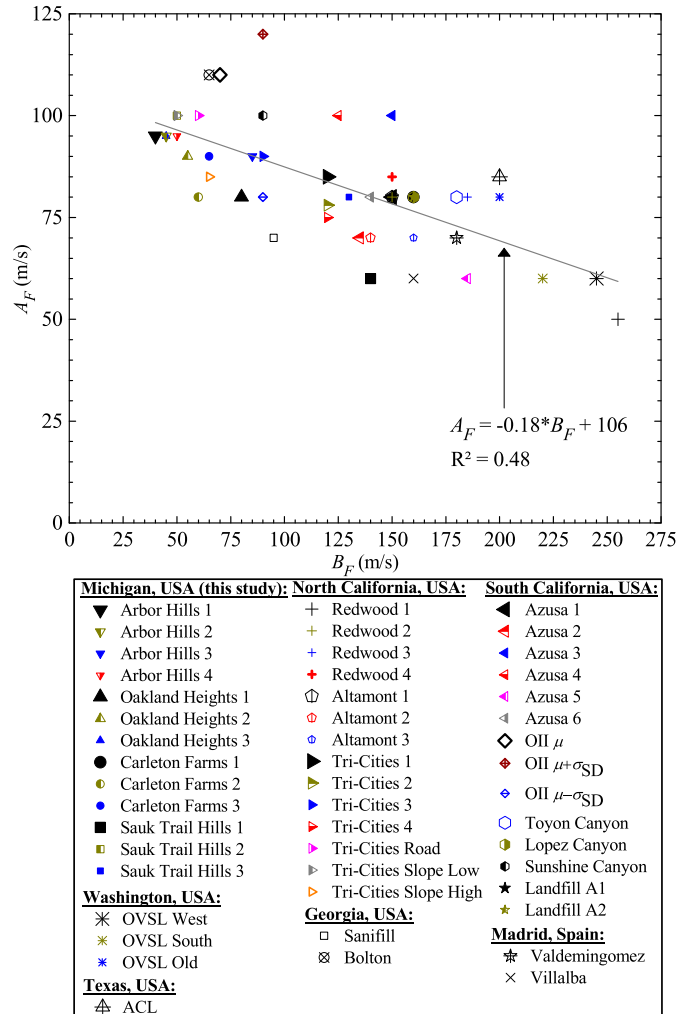
**Fig. 8.** Examples of measured  $V_s$  and modeled  $V_s$  profiles at various sounding locations from the literature and this study: (a–c) good model fits; (d and e) model fits with the misfit as a result of thin or thick crust; (f) poor model fit at several depths



**Fig. 9.** Statistics for the (a)  $A_F$  and (b)  $B_F$  calibration parameters

**Table 4.** Statistics of Regressed  $A_F$ ,  $B_F$ ,  $V_{si}$ ,  $\alpha_{V_s}$ , and  $\beta_{V_s}$  Parameters Based on Regression of Field Data

Method	Parameter	Mean ( $\mu$ )	Median	SD ( $\sigma_{SD}$ )	Maximum	Minimum
Semiempirical [Eq. (8)]	$A_F$ (m/s)	83	80	15	120	50
	$B_F$ (m/s)	124	130	56	255	40
Fully empirical [Eq. (10)]	$V_{si}$ (m/s)	89	85	21	158	48
	$\alpha_{V_s}$ (s)	0.08	0.07	0.04	0.19	0.04
	$\beta_{V_s}$ (s/m)	0.006	0.005	0.003	0.012	0.003

**Fig. 10.** Relationship between  $A_F$  and  $B_F$  based on field data

Theoretically, higher  $B_F$  parameters would be expected to be correlated with lower  $A_F$  parameters, meaning that when the  $V_s$  value near the surface is low (i.e.,  $A_F$  takes low values, in the order of 50–75 m/s), the increase in  $V_s$  with depth is significant (i.e.,  $B_F$  is high). The statistics of the empirical  $V_{si}$ ,  $\alpha_{V_s}$ , and  $\beta_{V_s}$  parameters are also shown in Table 4.

### Model Recommendations and Limitations

To develop a  $V_s$  profile using the semiempirical model [Eq. (8)] the parameters listed in Table 4 are needed. To use Eq. (8), an assumption for the variation of unit weight with depth needs to be made first. The Zekkos et al. (2006) procedures to measure in situ the unit weight profile can be used and in the absence of site-specific data,

the recommendations for low, typical, and high unit weight profiles (also shown in Table 3) can be used.

The recommended  $V_s$  profiles with depth using the semiempirical model are shown in Fig. 11 along with all field  $V_s$  profiles. Curves are shown for the mean  $V_s$  profiles using a typical unit weight profile, as well as using the high and low unit weight profiles, as recommended by Zekkos et al. (2006). Use of the typical unit weight profile with the  $\mu \pm \sigma_{SD}$  values for the  $A_F$  and  $B_F$  parameters generally bounds most of the field data with the exception of the  $V_s$  in the top 5 m. When site-specific data indicate that the unit weight of the MSW is higher or lower than the typical unit weight, a  $V_s$  profile can be developed considering the site-specific variation in unit weight. The present database does not include any sites with  $V_s$  profiles where the low unit weight profile was used. However, the  $V_s$  estimates of the semiempirical model for low unit weight profiles are shown and represent the lower bound of the data.

Fig. 11 only extends to a depth of 30 m where most field  $V_s$  data on MSW are available. Limited field data (e.g.,  $V_s$  profiles from the OII landfill) extend deeper. Because the mathematical expression of the semiempirical model was developed based on laboratory data for a range of confining stresses and the analyses confirmed that the derived  $A_F$  and  $B_F$  values are not depth/stress dependent, it would be expected that the semiempirical model estimates will be appropriate at greater depths as well.

The mathematically simpler, empirical model that is only a function of depth may be used instead of the semiempirical model. For the empirical model, Eq. (10) should be used along with the  $V_{si}$ ,  $\alpha_{V_s}$ , and  $\beta_{V_s}$  parameters given in Table 4. As shown in Fig. 12, the mean  $V_s$  profile for the empirical model is very similar to the mean  $V_s$  profile of the semiempirical model for the typical unit weight profile case. The lower- and upper-bound ( $\mu \pm \sigma_{SD}$ )  $V_s$  profiles for the empirical model are also similar but not identical to the  $\mu \pm \sigma_{SD}$   $V_s$  profiles of the semiempirical model for the typical unit weight profile case.

The models are not intended to capture the crust or other special fill and soil materials disposed of at some landfill locations. Based on the available field data, the crust may vary in thickness up to approximately 4 m and has  $V_s$  values on the order of 150–250 m/s. However, its presence and extent is site specific and dependent on a number of factors, including the type of soil, moisture content (and its fluctuation), and compaction effort. The presence of this high-velocity layer near the surface may impact the near-surface seismic response of the landfill. In that case, this high-velocity layer at the surface could be added and replace the model estimates of  $V_s$ .

The proposed models are also not intended to replace field measurements. As shown in Fig. 12, there are differences in the mean  $V_s$  profiles of MSW landfills from various regions (e.g., Michigan, southern California, and northern California). These geographic differences may be attributed to differences in waste streams; waste composition; climatic conditions (temperature and precipitation); and landfill operation practices such as the amount of compaction effort and daily soil cover used as well as the type of soil used for the daily soil cover. In the absence of any site-specific information, the models can be used as a basis for preliminary assessments of  $V_s$

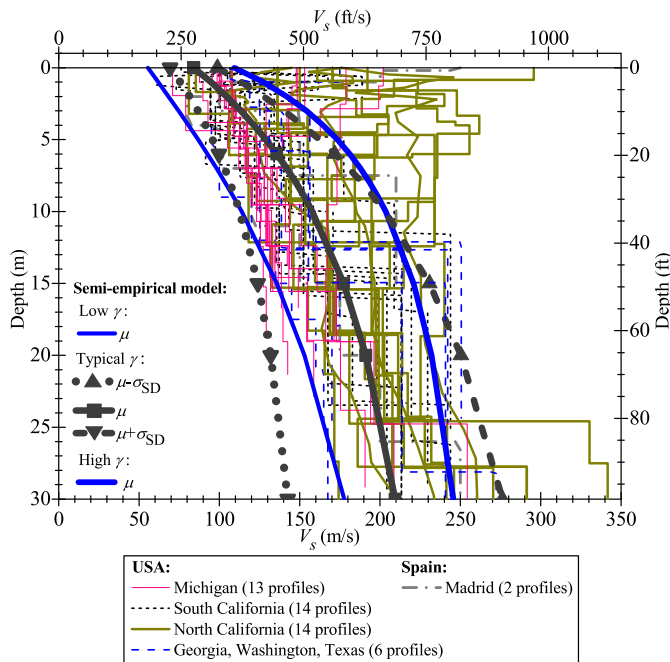


Fig. 11. Recommended shear-wave profiles from field data

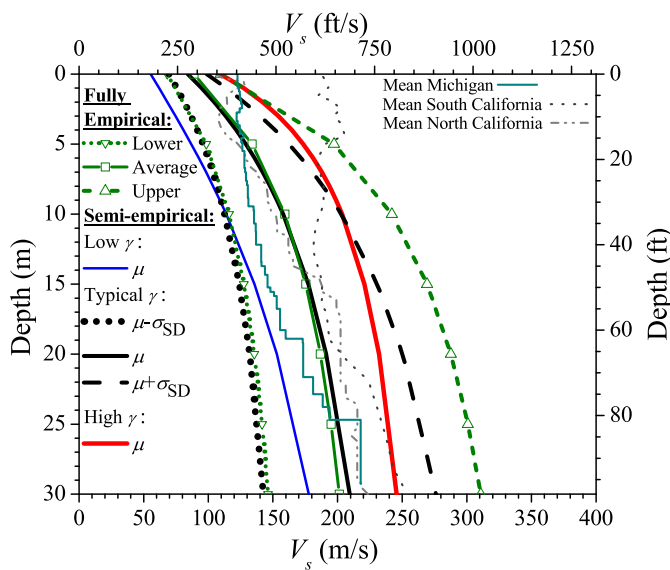


Fig. 12. Regressed semiempirical and fully empirical  $V_s$  profiles

and  $G_{max}$  of MSW. For example, in the absence of any information on the MSW, the mean curves of the empirical and semiempirical models can be recommended, and the model parameters are given in Table 4. However, as indicated by the SDs of the model parameters, there can be significant differences in the  $V_s$  profiles for various assumed model parameters. These differences can have a significant effect on the seismic response and seismic stability of the MSW landfill. Thus, any information about the MSW and the landfill operation practices (e.g., amount of compaction effort and amount of daily soil cover used) may help in the selection of the best-estimate  $V_s$  profile. Parametric analyses to assess the influence of the uncertainty in  $V_s$  on the seismic analysis results, as quantified by this study, may be necessary.

The models are also not suited to predict large, abrupt changes in  $V_s$  that are caused by the disposal of various waste or soil materials. It is also important to mention that most landfills included in the database and used to calibrate the models are modern dry tomb landfills, and thus the waste is not saturated. At old, abandoned landfills or bioreactor landfills, the waste may be in a nearly saturated condition and the validity of these models needs to be investigated.

## Conclusions

The  $V_s$  and associated  $G_{max}$  of MSW are important engineering properties and are crucial in evaluating the seismic response of landfills. Using insights gained from large-scale laboratory tests on reconstituted MSW specimens, a semiempirical model for  $V_s$  was developed. A hyperbolic function was used to describe the relationship of  $V_s$  with the effective confining stress (isotropic for the laboratory; vertical for field data) and a power function was used to describe the relationship of  $V_s$  with the unit weight of MSW. Based on the results from previous research studies, the unit weight of MSW was used to capture the effects of waste composition as well as compactness. Alternatively, a simpler empirical model that is only a function of depth was presented. Both models were calibrated against a total of 49 in situ  $V_s$  profiles in MSW. Thirty-six  $V_s$  profiles from 15 landfills in Georgia, southern California, northern California, Washington, Texas, and Spain that are available in the literature were used. The literature database was expanded with 13 additional profiles generated as part of this study from four landfills in Michigan. The models do not consider the crust effect or other unusual soil materials that may be present in a landfill and that can cause significant deviations from estimates using the model. Also, the models are not intended to replace in situ measurements but are intended to be used in preliminary assessments of the shear-wave velocity of MSW for design purposes.

## Acknowledgments

This paper is based upon field work supported by the National Science Foundation Division of Civil and Mechanical Systems under Grant No. CMMI-1041566 and earlier laboratory work supported by the National Science Foundation Division of Civil and Mechanical Systems under Grant Nos. CMMI-0220064 and CMMI-0219834. Any opinions, findings, conclusions, and recommendations expressed in this paper are those of the authors and do not necessarily reflect the views of the National Science Foundation. Additional information about this research project is available on the project's GeoWorld website (<http://www.mygeoworld.info>).

## References

- Aki, K. (1957). "Space and time spectra of stationary stochastic waves, with special reference to micro-tremors." *Bull. Earthquake Res. Inst., Univ. Tokyo*, 35, 415–456.
- Andrus, R. D., and Stokoe, K. H., II. (2000). "Liquefaction resistance of soils from shear-wave velocity." *J. Geotech. Geoenviron. Eng.*, 10.1061/(ASCE)1090-0241(2000)126:11(1015), 1015–1025.
- Asten, M. W., Dhu, T., and Lam, N. (2004). "Optimised array design for microtremor array studies applied to site classification; observations, "results and future use." *Proc., 13th World Conf. of Earthquake Engineering*, International Association for Earthquake Engineering, Tokyo.
- Athanasopoulos, G., Grizi, A., Zekkos, D., Founta, P., and Zisimatou, E. (2008). "Municipal solid waste as a reinforced soil: Investigation using synthetic waste." *Geotecnics of waste management*.

- and remediation, M. V. Khire, A. N. Alshawabkeh, and K. R. Reddy, eds., ASCE, Reston, VA, 168–175.
- Athanasopoulos-Zekkos, A., Zekkos, D., and Matasovic, N. (2008). "Validation of generic municipal solid waste material properties for seismic design of landfills." *Proc., 4th Geotechnical Earthquake Engineering and Soil Dynamics Conf*, ASCE, Reston, VA, 1–10.
- Augello, A. J., Bray, J. D., Leonards, G. A., Repetto, P. C., and Byrne, R. J. (1995). "Response of landfills to seismic loading." *Proc., Geoenvironment 2000*, Geotechnical Special Publication No. 46, Vol. 2, ASCE, New York, 1050–1065.
- Bellotti, R., Jamiolkowski, M., Lo Presti, D. C. F., and O'Neill, D. A. (1996). "Anisotropy of small-strain stiffness of Ticino Sand." *Geotechnique*, 46(1), 115–131.
- Bray, J. D., Zekkos, D., Kavazanjian, E., Jr., Athanasopoulos, G. A., and Riemer, M. F. (2009). "Shear strength of municipal solid waste." *J. Geotech. Geoenviron. Eng.*, 10.1061/(ASCE)GT.1943-5606.0000063, 709–722.
- Cox, B. R., and Beekman, A. N. (2011). "Intramethod variability in ReMi dispersion and  $V_s$  estimates at shallow bedrock sites." *J. Geotech. Geoenviron. Eng.*, 10.1061/(ASCE)GT.1943-5606.0000436, 354–362.
- Cuellar, V., Monte, J. L., and Valerio, J. (1998). "Static and dynamic elastic moduli for waste landfills." *Proc., 3rd Int. Congress on Environmental Geotechnics*, Vol. 1, Balkema, Amsterdam, Netherlands, 325–329.
- Dobry, R., and Vucetic, M. (1987). "State of the art report: Dynamic properties and response of soft clay deposits." *Proc., Int. Symp. on Geotechnical Engineering of Soft Soils*, Vol. 2, 51–87.
- Foti, S., Comina, C., Boiero, D., and Socco, L. V. (2009). "Non-uniqueness in surface-wave inversion and consequences on seismic site response analyses." *Soil Dyn. Earthquake Eng.*, 29(6), 982–993.
- Gucunski, N., and Woods, R. D. (1992). "Numerical simulation of the SASW test." *Soil Dyn. Earthquake Eng.*, 11(4), 213–227.
- Hanson, J. L., Yesiller, N., and Oettle, N. K. (2010). "Spatial and temporal temperature distributions in municipal solid waste landfills." *J. Environ. Eng.*, 10.1061/(ASCE)JEE.1943-7870.0000202, 804–814.
- Hardin, B. O. (1978). "The nature of stress-strain behavior for soils." *Proc., ASCE Geotechnical Engineering Division Specialty Conf. on Earthquake Engineering and Soil Dynamics*, Vol. 1, ASCE, New York, 3–90.
- Hardin, B. O., and Black, W. L. (1968). "Vibration modulus of normally consolidated clay." *J. Soil Mech. and Found. Div.*, 94(2), 353–370.
- Hardin, B. O., and Drnevich, V. P. (1972). "Shear modulus and damping in soil, measurement and parameter effects." *J. Soil Mech. and Found. Div.*, 98(6), 603–624.
- Hardin, B. O., and Richart, F. E., Jr. (1963). "Elastic wave velocities in granular soils." *J. Soil Mech. and Found. Div.*, 89(1), 33–65.
- Hryciw, R. D., and Thomann, T. G. (1993). "Stress-history-based model for  $G^e$  of cohesionless soils." *J. Geotech. Eng.*, 10.1061/(ASCE)0733-9410(1993)119:7(1073), 1073–1093.
- Iwasaki, T., and Tatsuoka, F. (1977). "Effects of grain size and grading on dynamic shear moduli of sands." *Soils Found.*, 17(3), 19–35.
- Kavazanjian, E., Jr. (1999). "Seismic design of solid waste containment facilities." *Proc., 8th Canadian Conf. on Earthquake Engineering*, 51–89.
- Kavazanjian, E., Jr., and Matasovic, N. (1995). "Seismic analysis of solid waste landfills." *Proc., GeoEnvironment 2000*, Geotechnical Special Publication No. 46, Vol. 2, ASCE, New York, 1066–1080.
- Kavazanjian, E., Jr., Matasovic, N., Bonaparte, R., and Schmertmann, G. R. (1995). "Evaluation of MSW properties for seismic analysis." *Proc., Geoenvironment 2000*, Geotechnical Special Publication No. 46, Vol. 2, ASCE, New York, 126–141.
- Kavazanjian, E., Jr., Matasovic, N., Stokoe, K. H., II, and Bray, J. D. (1996). "In situ shear wave velocity of solid waste from surface wave measurements." *Environmental geotechnics*, Vol. 1, M. Kamon, ed., Balkema, Rotterdam, Netherlands, 97–102.
- Kokusho, T., Yoshida, Y., and Essahi, Y. (1982). "Dynamic soil properties of soft clay for wide strain range." *Soils Found.*, 22(4), 1–18.
- Kramer, S. L. (1994). *Geotechnical earthquake engineering*, Prentice Hall, Upper Saddle River, NJ.
- Lee, J. J. (2007). "Dynamic characteristics of municipal solid waste (MSW) in the linear and nonlinear strain ranges." Ph.D. dissertation, Univ. of Texas at Austin, Austin, TX.
- Lin, Y.-C., Rosenblad, B., and Stokoe, K. H., II. (2004). "Data report on shear wave velocity profiles determined by SASW method at: Altamont landfill, Redwood landfill, and Tri-Cities landfill." *Geotechnical Engineering Rep. GR04-3*, Geotechnical Engineering Center, Dept. of Civil and Environmental Engineering, Univ. of Texas at Austin, Austin, TX.
- Matasovic, N., and Kavazanjian, E., Jr. (1998). "Cyclic characterization of OII landfill solid waste." *J. Geotech. Geoenviron. Eng.*, 10.1061/(ASCE)1090-0241(1998)124:3(197), 197–210.
- Matasovic, N., and Kavazanjian, E., Jr. (2006). "Seismic response of a composite landfill cover." *J. Geotech. Geoenviron. Eng.*, 10.1061/(ASCE)1090-0241(2006)132:4(448), 448–455.
- Menq, F.-Y. (2003). "Dynamic properties of sandy and gravelly soils." Ph.D. thesis, Univ. of Texas at Austin, Austin, TX.
- Okada, H. (2003). *The microtremor survey method*, Geophysical Monograph Series No. 12, Society of Exploration Geophysicists, Tulsa, OK.
- Park, C. B., et al. (2004). "Imaging dispersion curves of passive surface waves." *SEG technical program expanded abstracts 2004*, Society of Exploration Geophysicists, Tulsa, OK, 1357–1360.
- Park, C. B., Miller, R. D., and Xia, J. (1999a). "Multichannel analysis of surface wave." *Geophysics*, 64, 800–808.
- Park, C. B., Miller, R. D., and Xia, J. (1999b). "Multimodal analysis of high frequency surface wave." *Proc., Symp. on the Application of Geophysics to Engineering and Environmental Problems (SAGEEP 99)*, Environmental and Engineering Geophysical Society, Wheat Ridge, CO, 115–122.
- Pelekis, P. C., and Athanasopoulos, G. A. (2011). "An overview of surface wave methods and a reliability study of a simplified inversion technique." *Soil Dyn. Earthquake Eng.*, 31(12), 1654–1668.
- Pereira, A. G. H., Sopena, L., and Mateos, T. G. (2002). "Compressibility of a municipal solid waste landfill." *Proc., 4th Int. Congress on Environmental Geotechnics*, Balkema, Amsterdam, Netherlands 201–206.
- Richart, F. E., Jr. (1975). "Some effects of dynamic soil properties on soil-structure interaction." *J. Geotech. Eng. Div.*, 101(12), 1193–1240.
- Rix, G. J., Lai, C. G., Foti, S., and Zywicki, D. (1998). "Surface wave tests in landfills and embankments." *Geotechnical earthquake engineering and soil dynamics III*, Geotechnical Special Publication No. 75, Vol. 2, ASCE, New York, 1008–1019.
- Rosenblad, B. L., Li, J., Menq, F.-Y., and Stokoe, K. H., II. (2007). "Deep shear wave velocity profiles from surface wave measurements in the Mississippi Embayment." *Earthquake Spectra*, 23(4), 791–809.
- Sahadewa, A., Zekkos, D., Lobbstaal, A., and Woods, R. D. (2011). "Shear wave velocity of municipal solid waste in Michigan landfills." *Proc., 14th Pan-American Conf. on Soil Mechanics and Geotechnical Engineering and 64th Canadian Geotechnical Conf. on Geo-Innovation Addressing Global Challenges (CD-ROM)*, The Canadian Geotechnical Society, Richmond, BC, Canada.
- Sahadewa, A., Zekkos, D., and Woods, R. D. (2012). "Observations from the implementation of a combined active and passive surface wave based methodology." *Proc., State of the Art and Practice in Geotechnical Engineering Conf. (Geotronics 2012)*, ASCE, Reston, VA, 2786–2795.
- Seed, H. B., and Idriss, I. M. (1970). "Soil moduli and damping factors for dynamic response analyses." *Rep. No. EERC 70-10*, Univ. of California at Berkeley, Berkeley, CA.
- Sharma, H. D., Dukes, M. T., and Olsen, D. M. (1990). "Field measurements of dynamic moduli and Poisson's ratios of refuse and underlying soils at a landfill site." *Geotechnics of waste fills—Theory and practice, STP 1070*, A. Landva and G. D. Knowles, eds., ASTM, West Conshohocken, PA, 57–70.
- Sheehan, A. J., Olson, R. E., Park, K., and Stokoe, K. H., II. (2010). "Estimation of settlement of footings under working loads using equivalent-linear elasticity." *GeoFlorida 2010: Advances in analysis, modeling & design (CD-ROM)*, ASCE, Reston, VA, 1708–1717.
- Singh, S., and Murphy, B. J. (1990). "Evaluation of the stability of sanitary landfills." *Geotechnics of waste fills—Theory and practice, STP 1070*, A. Landva and G. D. Knowles, eds., ASTM, West Conshohocken, PA, 240–257.
- Stokoe, K. H., II, Lee, J. N.-K., and Lee, S. H.-H. (1991). "Characterization of soil in calibration chambers with seismic waves." *Proc., 1st Int. Symp. on Calibration Chamber Testing*, Elsevier, New York.
- Stokoe, K. H., II, and Santamarina, J. C. (2000). "Seismic-wave-based testing in geotechnical engineering." *Proc., Int. Conf. on Geotechnical*

- and *Geological Engineering (GeoEng 2000)*, Vol. 1, Technomic Publishing, Lancaster, PA, 1490–1536.
- Stokoe, K. H., II, Wright, S. G., Bay, J. A., and Roesset, J. M. (1994). “Characterization of geotechnical sites by SASW method.” *Geophysical characterization of sites*, R. Woods, ed., International Science, New York, 15–26.
- Strobbia, C., and Cassiani, G. (2011). “Refraction microtremors: Data analysis and diagnostics of key hypotheses.” *Geophysics*, 76(3), MA11–MA20.
- Tokimatsu, K., Tamura, S., and Kojima, H. (1992). “Effects of multiple modes of Rayleigh wave dispersion characteristics.” *J. Geotech. Engrg.*, 10.1061/(ASCE)0733-9410(1992)118:10(1529), 1529–1543.
- Tran, K. T., and Hiltunen, D. R. (2008). “A comparison of shear wave velocity profiles from SASW, MASW, and ReMi techniques.” *Geotechnical earthquake engineering and soil dynamics IV, GSP 181* (CD-ROM), ASCE, Reston, VA.
- Xia, J., Miller, R. D., and Park, C. B. (1999). “Estimation of near-surface shear wave velocity by inversion of Rayleigh waves.” *Geophysics*, 64(3), 691–700.
- Yoon, S., and Rix, J. G. (2009). “Near-field effects on array-based surface wave methods with active sources.” *J. Geotech. Geoenviron. Eng.*, 10.1061/(ASCE)1090-0241(2009)135:3(399), 399–406.
- Youd, T. L., et al. (2001). “Liquefaction resistance of soils: Summary report from the 1996 NCEER and 1998 NCEER/NSF workshops on evaluation of liquefaction resistance of soils.” *J. Geotech. Geoenviron. Eng.*, 10.1061/(ASCE)1090-0241(2001)127:10(817), 817–833.
- Yuan, P., Kavazanjian, E., Jr., Chen, W., and Seo, B. (2011). “Compositional effects on the dynamic properties of municipal solid waste.” *Waste Manage.*, 31(12), 2380–2390.
- Zalachoris, G. (2010). “Field measurements of linear and nonlinear shear moduli of solid municipal waste using a dynamically loaded surface footing.” M.S. thesis, Univ. of Texas at Austin, Austin, TX.
- Zekkos, D., et al. (2006). “Unit weight of municipal solid waste.” *J. Geotech. Geoenviron. Eng.*, 10.1061/(ASCE)1090-0241(2006)132:10(1250), 1250–1261.
- Zekkos, D., Bray, J. D., and Riemer, M. F. (2008). “Shear modulus and material damping of municipal solid waste based on large-scale cyclic triaxial testing.” *Can. Geotech. J.*, 45(1), 45–58.
- Zekkos, D., Kavazanjian, E., Jr., Bray, J. D., Matasovic, N., and Riemer, M. F. (2010). “Physical characterization of municipal solid waste for geotechnical purposes.” *J. Geotech. Geoenviron. Eng.*, 10.1061/(ASCE)GT.1943-5606.0000326, 1231–1241.
- Zekkos, D., Matasovic, N., El-Sherbiny, R., Athanasopoulos-Zekkos, A., Towhata, I., and Maugeri, M. (2011). “Dynamic properties of municipal solid waste.” *Geotechnical characterization, field measurement, and laboratory testing of municipal solid waste*, Geotechnical Special Publication No. 209, D. Zekkos, ed., ASCE, Reston, VA, 112–134.
- Zekkos, D. P. (2005). “Evaluation of static and dynamic properties of municipal solid-waste.” Ph.D. dissertation, Dept. of Civil and Environmental Engineering, Univ. of California at Berkeley, Berkeley, CA.
- Zhou, Y., and Chen, Y. (2005). “Influence of seismic cyclic loading history on small strain shear modulus of saturated sands.” *Soil Dyn. Earthquake Eng.*, 25(5), 341–353.

Copyright of Journal of Geotechnical & Geoenvironmental Engineering is the property of American Society of Civil Engineers and its content may not be copied or emailed to multiple sites or posted to a listserv without the copyright holder's express written permission. However, users may print, download, or email articles for individual use.